Available online at www.sciencedirect.com

SciVerse ScienceDirect

Ceramics International 39 (2013) 2259–2265

CERAMICS INTERNATIONAL

www.elsevier.com/locate/ceramint

Effects of electron-beam irradiation, a thin-Ti layer, and a BeO additive on the diffusion of titanium in synthetic sapphire

Yongkil Ahn[a], Jingyo Seo[a], Pornsawat Wathanakul[b,c], Jongwan Park[a,*]

[a]Department of Materials Science and Engineering, Hanyang University, 17 Haengdang-dong, Seongdong-gu, Seoul 133-791, Republic of Korea
[b]Department of Earth Sciences, Faculty of Science, Kasetsart University, Bangkok 10900, Thailand
[c]The Gem and Jewelry Institute of Thailand (Public Organization), Bangkok 10500, Thailand

Received 29 July 2012; received in revised form 23 August 2012; accepted 23 August 2012
Available online 6 September 2012

Abstract

Titanium was allowed to diffuse into synthetic sapphire (α-Al_2O_3) at 1773–1923 K for 200 h in air. Specimens were prepared by four different methods. Samples were irradiated with a 10 MeV electron beam to fluencies of 2×10^{17} cm^{-2} for 1 h to induce vacancy formation. A 1-μm layer of titanium was sputtered onto sapphire samples to provide intimate contact with the diffusing elements. Ti diffusion was performed using TiO_2 powder or a mixture of TiO_2 and BeO powders in a ratio of 95:5 to take advantage of the beryllium activity. Ti diffusion was profiled using scanning electron microscope-energy dispersive X-ray spectrometry (SEM–EDX). The diffusion coefficients of Ti were as follows:

Sapphire irradiated, coated with Ti, and embedded in TiO_2/BeO mixture.
$D_{Ti} = 1.9\exp\ (-572.1 \pm 18.5\ kJ\ mol^{-1}/RT)\ m^2\ s^{-1}$,
Sapphire irradiated, coated with Ti, and embedded in TiO_2 powder.
$D_{Ti} = 1.4\exp\ (-577.4 \pm 23.3\ kJ\ mol^{-1}/RT)\ m^2\ s^{-1}$,
Sapphire irradiated, non-coated and, embedded in TiO_2 powder.
$D_{Ti} = 1.2\exp\ (-582.4 \pm 27.1\ kJ\ mol^{-1}/RT)\ m^2\ s^{-1}$,
Sapphire non-irradiated, non-coated, and embedded in TiO_2 powder.
$D_{Ti} = 9.0\exp\ (-621.4 \pm 12.4\ kJ\ mol^{-1}/RT)\ m^2\ s^{-1}$

These results demonstrate that titanium penetrated the deepest into the sapphire samples that were electron-beam-irradiated, coated with Ti, and embedded in the TiO_2/BeO mixture.

Keywords: C. Diffusion; D. Al_2O_3; D. TiO_2; Electron beam irradiation

1. Introduction

Corundum (α-Al_2O_3) can produce gemstones of various colors depending on the impurity atoms substituted at the Al sites. Among these, ruby and blue sapphires are precious gemstones. The crystal structure of corundum belongs to the space group D^6_{3d}, and the rhombohedral unit cell is composed of two Al_2O_3 species. The aluminum cations are linked to 6 oxygen anions in a distorted octahedron, which is about two-thirds full [1]. The ionic radius of the impurities is larger than the aluminum atom, i.e., $Cr^{3+} = 0.615$ Å, $Fe^{3+} = 0.645$ Å, $Ti^{4+} = 0.605$ Å, compared with $Al^{3+} = 0.535$ Å, in an octahedral site [2]. Ti-doped sapphires can be used in tunable solid-state lasers. These lasers emit red and near-infrared light in the range of 650–1100 nm [3]. The red color of rubies is attributed to 1000 ppma Cr^{3+}, and 50 ppma Fe^{2+}–Ti^{4+} pairs are responsible for the deep blue color of sapphires [4]. The Ti^{4+} ion is slightly larger than Al^{3+}, therefore it easily enters the corundum lattice. If Fe^{2+} and Ti^{4+} ions are located adjacent to Al sites, they interact, adjusting the ionic valence of the structure. Specifically, Fe^{2+} is converted to Fe^{3+} by losing 1 electron, and Ti^{4+} is altered to Ti^{3+} by receiving 1 electron: $Fe^{2+} + Ti^{4+} \rightarrow$

*Corresponding author. Tel.: +82 2 2220 0386; fax: +82 2 2298 2850.
E-mail address: jwpark@hanyang.ac.kr (J. Park).

0272-8842/$ - see front matter © 2012 Elsevier Ltd and Techna Group S.r.l. All rights reserved.
http://dx.doi.org/10.1016/j.ceramint.2012.08.071

$Fe^{3+}+Ti^{3+}$. This process is called intervalence charge transfer (IVCT). In corundum, IVCT requires about 2.11 eV. Consequently, the absorption band at 588 nm contributes to the blue color [5].

Our previous research on the diffusion of Cr^{3+} ions in sapphire [6] found that Cr-coating and electron beam irradiation yielded the deepest penetration of Cr^{3+} ions among the three methods evaluated: coated and electron beam irradiated, electron beam irradiated only, and non-irradiated. The coating method overlaid a uniform chromium film 1 μm thick on the sapphire surface using an evaporator.

In the present work, we studied titanium diffusion in sapphire. Following our previous work, we used three methods to diffuse titanium into sapphire. Additionally, we tried mixing titanium oxide powder with beryllium oxide powder as an additive to enhance penetration. The diffusion coefficient of Be^{2+} ions in corundum was estimated to be about 10^{-11} m^2/s at 2023 K [4]. For each case, we measured the diffusion coefficients and diffusivities [$D=D_0\ exp\ (-Q_d/RT)$] of titanium in sapphire. Finally, we compared the diffusion kinetics of the four cases using the activation energies for diffusion obtained from the calculated diffusivities.

2. Experimental procedures

Diffusion was carried out using synthetic sapphire samples. The synthetic colorless sapphire was obtained from Hrand Djevahirdjian SA (Djeva) Ltd. in Monthey, Switzerland. Specimens were cut perpendicularly in the growth direction. Samples were sliced into 16 square pieces using a diamond sawing machine. Each sample was $10\times10\times2$ mm^3. The surfaces were polished using three methods: silicon carbide cc-220 cw, cc-2000 cw abrasive paper, and alumina powder. The polished sapphires were then cleaned for 10 min in an ultrasonic bath filled with distilled water [7].

For comparison with our previous study, we pre-irradiated 12 pieces of sapphire in an electron accelerator at an electron energy of 10 MeV to fluencies of 2×10^{17} cm^{-2}. A 1 μm-thick titanium layer was coated by evaporation onto the sapphire surfaces after electron beam irradiation. A columned lump of titanium metal was packed into a $1\times1\times1$ cm^3 carbon crucible. The titanium was melted and evaporated via electron beam using the following conditions: beam current of 60 mA, voltage of 4.36 kV, and a high vacuum pressure of 3×10^{-6} Torr.

We prepared two types of titanium for diffusion: titanium oxide powder for embedding and titanium metal for evaporation. For the Ti^{4+} ion doping, titanium oxide powder and titanium metal of 99.0% purity were purchased from Duksan Pure Chemical Co. Ltd., Korea. As an additive, BeO powder of 99.0% purity was purchased from A Johnson Matthey. Diffusion experiments were performed using sapphire samples prepared by four different preparation methods: with or without electron beam irradiation, with or without Ti coating on the sapphire surface, and with samples embedded in TiO_2 powder and a TiO_2 (95%)/BeO (5%) powder mixture. The specimens embedded in powder were tightly packed into an alumina ceramic crucible with a cover. The specimens were then heated in an electric furnace in a horizontal alumina tube. The heat treatment was conducted in 50 K intervals at temperatures ranging from 1773 K to 1923 K for 200 h in air. The temperature was steadily raised by 3 K a minute and quenched at 1673 K. Cross sections of the diffused specimens were ground and polished horizontally.

3. SEM-EDS and LA-ICP-MS analysis

Titanium diffusion in the samples was investigated using a scanning electron microscope (SEM; Nova Nano 200, FEI Co.). The depth profiles of diffused titanium were measured by energy dispersive X-ray spectrometry (EDX) (EDAX Inc.). Fig. 1 shows the positions of the detecting points on the cross-section of the diffused samples. To detect diffused elements, we measured the diffused content (ppma) of beryllium and titanium at these positions using a laser ablation inductively coupled plasma mass spectrometer (7500 series LA-ICP-MS, Agilent Technologies Company) at the Gem and Jewelry Institute of Thailand.

4. Results and discussion

Fig. 2 shows an SEM image of the sapphire samples after diffusion. The cross-sectioned surface of the sapphires was distinguished by Ti- and Al-rich oxide layers, along with the original interface. The highlighted horizontal line was used for line scanning by EDS. The depth profiles of diffused titanium were obtained by line-scanning from the highlighted line toward an aluminum-rich surface. We analyzed the titanium counts based on the depth profile from EDS.

Fig. 3 depicts the Ti profile in sapphire samples heated at 1773 K for 200 h. The Ti concentration versus diffusion depth (10^{-6} m) was consistent with a Gaussian-type distribution. Fig. 3 was converted into log (Ti counts) versus x^2 (square of

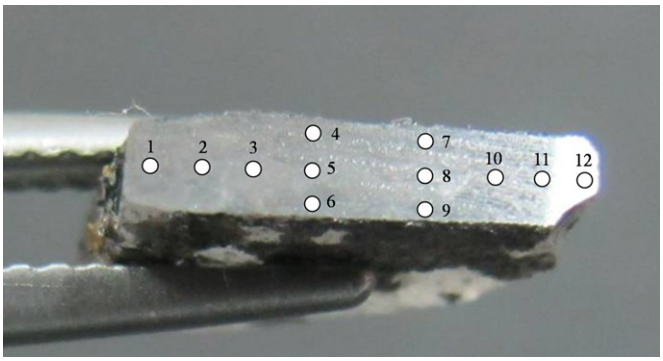

Fig. 1. Positions of the detecting points on the cross-section of the diffused samples measured by LA-ICP-MS.

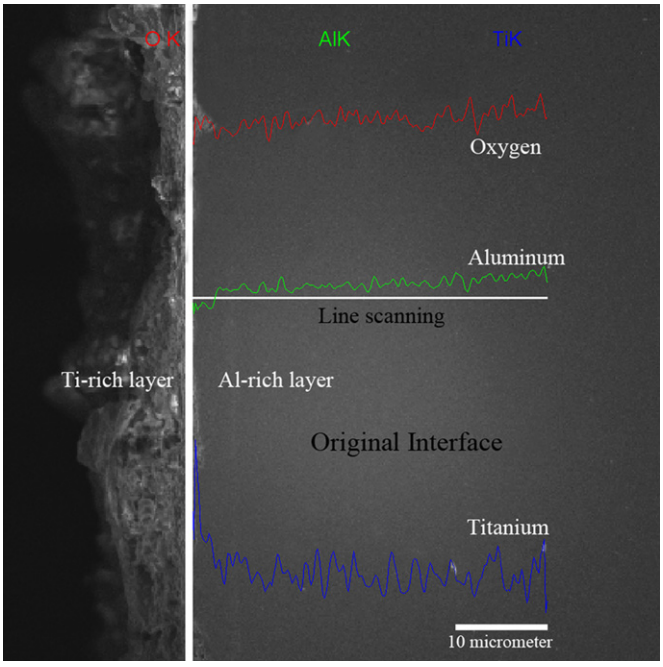

Fig. 2. Scanning electron microscope image of cross-sectioned titanium oxide (TiO_2)/sapphire (Al_2O_3) after diffusion treatment at 1773 K for 200 h.

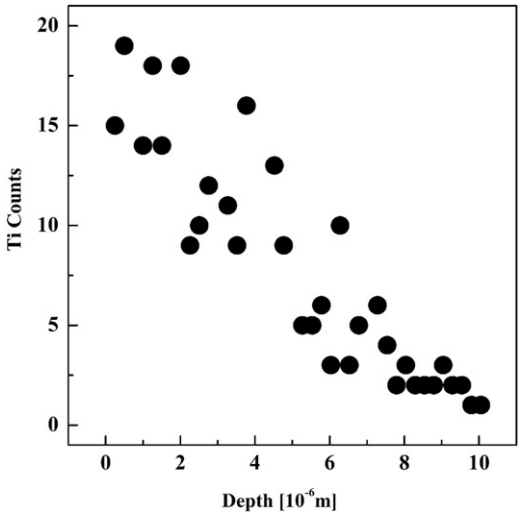

Fig. 3. Count profile of Ti in sapphire after diffusion at 1773 K for 200 h in air.

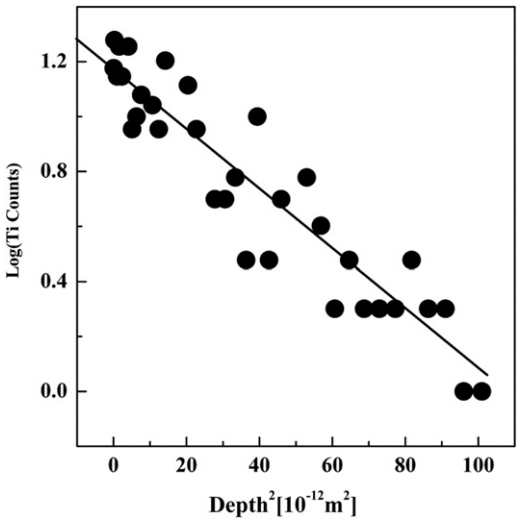

Fig. 4. Logarithm of the Ti counts versus the square of the diffusion depth from the data shown in Fig. 3.

Table 1
Diffusion data for Ti^{4+} in sapphire.

Sample no.	T (K)	$1/T$ (10^4/k)	T (s)	D ($m^2\,s^{-1}$)	log D
SST1	1773	5.64	7.2×10^5	4.075×10^{-18}	−17.390
SST2	1823	5.48	7.2×10^5	1.450×10^{-17}	−16.839
SST3	1873	5.34	7.2×10^5	3.769×10^{-17}	−16.424
SST4	1923	5.20	7.2×10^5	1.131×10^{-16}	−15.947
SST5	1773	5.64	7.2×10^5	7.935×10^{-18}	−17.100
SST6	1823	5.48	7.2×10^5	2.111×10^{-17}	−16.676
SST7	1873	5.34	7.2×10^5	6.910×10^{-17}	−16.161
SST8	1923	5.20	7.2×10^5	1.633×10^{-16}	−15.787
SST9	1773	5.64	7.2×10^5	1.371×10^{-17}	−16.863
SST10	1823	5.48	7.2×10^5	3.518×10^{-17}	−16.454
SST11	1873	5.34	7.2×10^5	1.055×10^{-16}	−15.977
SST12	1923	5.20	7.2×10^5	3.393×10^{-16}	−15.549
SST13	1773	5.64	7.2×10^5	2.450×10^{-17}	−16.611
SST14	1823	5.48	7.2×10^5	8.041×10^{-17}	−16.095
SST15	1873	5.34	7.2×10^5	2.154×10^{-16}	−15.667
SST16	1923	5.20	7.2×10^5	5.025×10^{-16}	−15.299

Sample no. SST1∼4 are pristine synthetic sapphires, SST5∼8 are synthetic sapphires irradiated with an electron beam, SST9∼12 are synthetic sapphires irradiated with an electron beam and then coated with Ti, and SST13∼16 are synthetic sapphires embedded in BeO/TiO_2 powder mixture under the same conditions as SST9∼12.

the diffusion depth), as shown in Fig. 4. The diffusion coefficient (D) was calculated by applying Fick's second law. The concentration function of a semi-infinite system can be defined as follows:

$$C(x,t) = \alpha/(\pi Dt)^{1/2}\exp(-x^2/4Dt) \quad (1)$$

This equation is a Gaussian exponential function, where $C(x, t)$ represents the Ti concentration as a function of the diffusion depth from the surface (x) and time (t). Fig. 4 depicts a simple one-dimensional function. The slope of the straight line is $-1/(2.303\times 4Dt)$. Therefore, the diffusion coefficient (D) is $-1/(2.303\times 4t\times$ slope) [8]. Table 1 shows the diffusion coefficients (D) and logarithm D data at each temperature for the samples pre-treated by the four different conditions.

In the surface analysis by SEM, we could barely detect sintered TiO_2 crystals on the sapphire surface. The absence of these crystals was due to rapid cooling from 1673 K after diffusion in the furnace. Even if some TiO_2 crystals grew on the sapphire surface, their morphology was significantly different from the Cr_2O_3 crystals that formed in our previous study [6]. Fig. 5 shows SEM images of the titanium and chromium crystals. Fig. 5(a) and (b) show

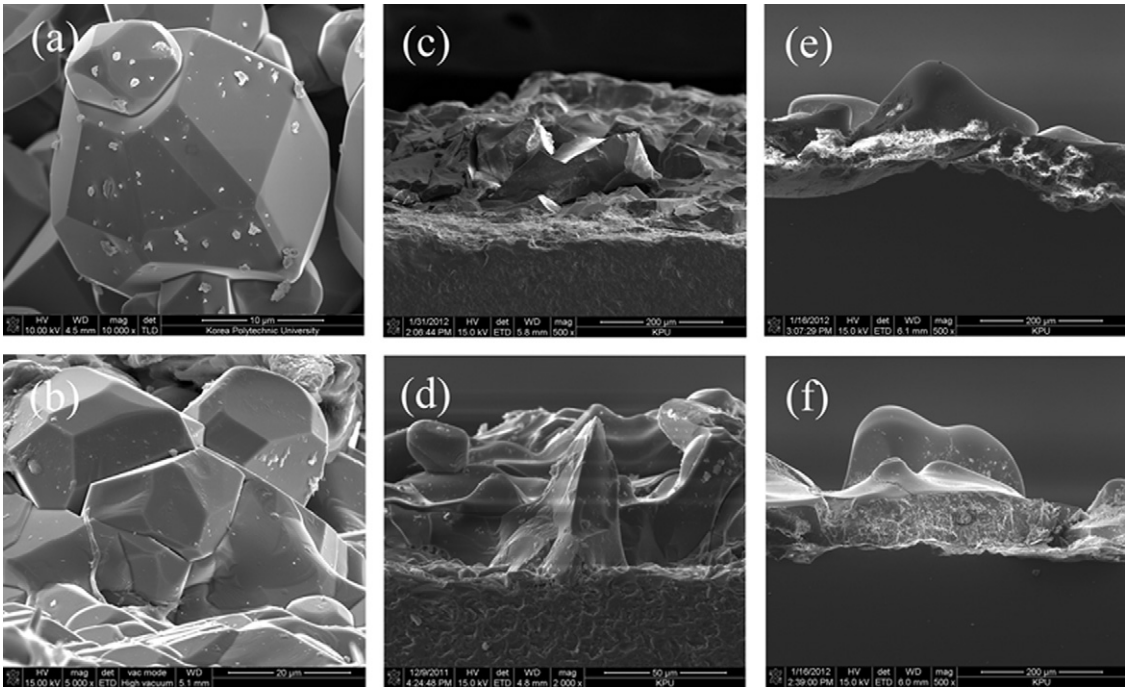

Fig. 5. SEM images of the crystal growth of chromium on the chrysoberyl surface after heating at 1773 K for 200 h (a) magnified 10,000× [12]. SEM images of the crystal growth of chromium on the sapphire surface after heating at 1823 K for 200 h (b) magnified 5000× [6]. SEM images of the crystal growth of titanium on the sapphire surface after heating at 1873 K for 200 h (c) magnified 500×, (d) magnified 2000×. SEM images of the crystal growth of titanium on the sapphire surface after heating at 1923 K for 200 h (e) and (f) magnified 500×.

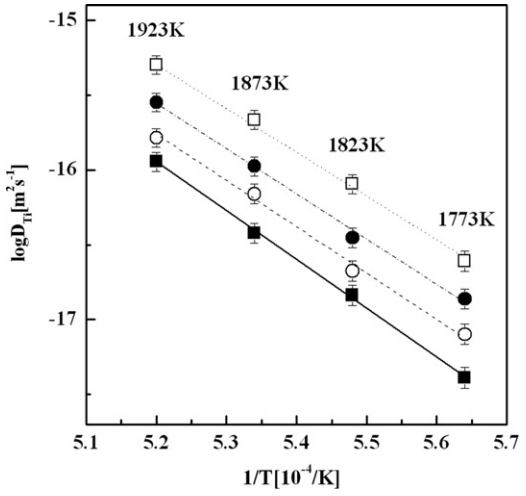

Fig. 6. Arrhenius plots of Ti diffusion into sapphire samples after heating at temperatures from 1773 to 1923 K for 200 h. The sample coated with Ti, irradiated, and embedded in TiO_2/BeO powder is marked by empty squares. The sample coated with Ti, irradiated, and embedded in TiO_2 powder is marked by filled circles. The sample that was non-coated, irradiated, and embedded in TiO_2 powder is marked by empty circles. The unmodified sample is marked by filled squares.

angular Cr_2O_3 crystals. The TiO_2 crystals were not angular, as shown in Fig. 5(c)–(f). The difference between the TiO_2 and Cr_2O_3 crystals seems to be due to the cooling method used.

To calculate the activation energies and pre-exponentials, the obtained diffusion coefficients were plotted against the reciprocal temperature ($1/T$), as shown in Fig. 6. The temperature dependence of the diffusivity can be determined as follows:

$$D = D_0\, exp(-Q_d/RT) \tag{2}$$

where D_0 (m^2/s) is the pre-exponential factor, Q_d (J/mol) is the activation energy, R [8.31 J/(mol K)] is the gas constant, and T (K) is the absolute temperature. Taking the logarithm of both sides of Eq. (2) gives:

$$In\ D = In\ D_0 - Q_d/R(1/T) \tag{3}$$

Substituting common logarithms for natural logarithms gives

$$Log\ D = log\ D_0 - Q_d/2.3R(1/T) \tag{4}$$

Therefore, the slope (α) is equal to $-Q_d/2.3R$ and the intercept (β) to log D_0 [9].

Using Eq. (4), we calculated Q_d and D_0 for each sample. From the data in Table 1 and Fig. 6, we obtained Arrhenius equations for the diffusion coefficient of Ti^{4+} in the temperature range of 1773–1923 K as follows:

Sapphire irradiated, coated with Ti, and embedded in a TiO_2/BeO mixture:

$$D_{Ti} = 1.9 \exp(-572.1 \pm 18.5\ \text{kJ mol}^{-1}/RT)\ \text{m}^2\ \text{s}^{-1},$$

Sapphire irradiated, coated with Ti, and embedded in TiO_2 powder:

$$D_{Ti} = 1.4 \exp(-577.4 \pm 23.3\ \text{kJ mol}^{-1}/RT)\ \text{m}^2\ \text{s}^{-1};$$

Sapphire irradiated, non-coated, and embedded in TiO_2 powder:

$$D_{Ti} = 1.2 \exp(-582.4 \pm 27.1 \text{ kJ mol}^{-1}/RT)\ \text{m}^2\ \text{s}^{-1};$$

Sapphire non-irradiated, non-coated, and embedded in TiO_2 powder:

$$D_{Ti} = 9.0 \exp(-621.4 \pm 12.4 \text{ kJ mol}^{-1}/RT)\ \text{m}^2\ \text{s}^{-1}.$$

These results imply that the titanium penetrated deepest into sapphires that were electron beam-irradiated, coated with Ti, and embedded in a mixture of TiO_2 and BeO powders.

We carried out diffusion experiments under four different conditions. Our previous work discusses the electron beam irradiation and surface coating methods in detail. An electron energy of 10 MeV allows electrons to penetrate up to 15 mm into the sample [10]. As such, the crystal structure develops many cation and anion vacancies. New F and V^{2-} centers form as well. Therefore, this process helps Ti^{4+} ions penetrate deeply into the crystal lattice. The non-irradiated samples were more structurally stable than irradiated samples, as there were fewer V^{2-} centers. Therefore, in non-irradiated sapphire samples, fewer Ti^{4+} ions penetrate the structure as compared with that of irradiated samples [11].

The coating method seems to play a considerable role in the diffusion process. We evenly evaporated titanium metal onto the sapphire surface. This coating technique provides good contact between the Ti source and the sample to efficiently supply the diffusion elements. Consequently, these methods resulted in deeper diffusion than the non-treated sapphires [6]. In this study, we also tried to embed samples in a mixture of TiO_2 (95%) and BeO (5%) powders during the diffusion treatment. Fig. 7 shows the diffusion of beryllium and titanium (ppma) at each sample position. We verified that more beryllium diffused to the center of the sapphire. Be^{2+} can deeply penetrate into the sapphire lattice, probably due to its small radius (0.27 Å) and faster ionization. During the diffusion treatment, beryllium from the TiO_2/BeO mixture began to enter the sapphire structure much faster and earlier than titanium through cation vacancies in the sapphire lattice formed by the electron beam irradiation. Therefore, Be^{2+} ions occupied the cation or interstitial sites first, and the remaining adjacent octahedral sites were then filled by Ti^{4+} ions. To achieve electrical neutrality in the crystals, cation vacancies in sapphire tend to accept trivalent cations due to the vacancies formed by missing Al^{3+} ions in the lattice. Because Be^{2+} ions enter the sapphire lattice during the heat treatment, 4^+ cations are needed for electrical neutrality. Therefore, Ti^{4+} ions tend to diffuse after Be^{2+} ions. Each diffused Ti^{4+} ion is captured by the lattice adjacent to a site occupied by a Be^{2+} ion, and the ions interact to adjust the ionic valence in the crystals, i.e., $Be^{2+} + Ti^{4+}$ share two Al^{3+} vacancies. Ti^{4+} ions continually diffuse into the lattice from the surface due to the concentration gradient. This diffusion may be interrupted if the diffused beryllium exits the lattice to the surface. As shown in Fig. 7, there was much more diffused beryllium at the center than at the surface of the sapphire. As shown in Fig. 8, titanium diffused better at higher temperatures.

Fig. 9 shows the diffusivities of titanium and chromium transition metals in the crystals. The diffusivity data from Ti were compared with that of Cr from the previous study [6]. At 1773 K ($1/T = 5.64 \times 10^{-4}\ \text{K}^{-1}$), the diffusion coefficients of Cr in sapphire were higher than in chrysoberyl [12], even though the diffusion rates were similar at 1923 K ($1/T = 5.20 \times 10^{-4}\ \text{K}^{-1}$). Furthermore, the Ti diffusivities in sapphire were considerably different from Cr in sapphire and chrysoberyl. At 1773 K, the diffusion coefficients ($\text{m}^2\,\text{s}^{-1}$) of Cr and Ti in non-irradiated sapphires were 2.899×10^{-19} and 4.075×10^{-18}, respectively. There is approximately one order of magnitude difference

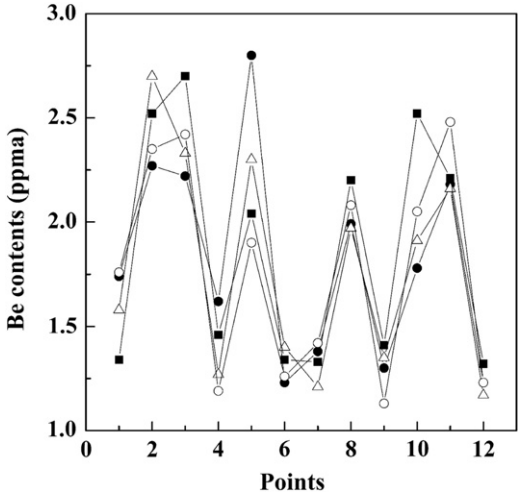

Fig. 7. The diffused contents (ppma) of beryllium at various positions in the sapphire that was irradiated, Ti coated, and embedded in a TiO_2/BeO powder mixture; 1923 K (empty circles), 1873 K (filled squares), 1823 K (empty triangle), and 1773 K (filled circles).

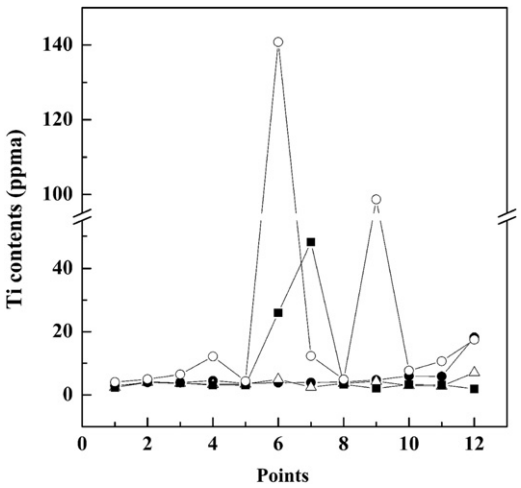

Fig. 8. The diffused contents (ppma) of the titanium at various positions in the sapphire that was irradiated, Ti coated, and embedded in a TiO_2/BeO mixture; 1923 K (empty circles), 1873 K (filled squares), 1823 K (empty triangle), and 1773 K (filled circles).

in the diffusion coefficients of Ti and Cr. This implies that Ti diffuses into the sapphire lattice more easily than Cr because the radius of the Ti^{4+} ion (0.605 Å) is smaller than the Cr^{3+} ion (0.615 Å). The slope of diffusivity, however, was lower for Cr diffusion (Table 2). Therefore, the activation energy for Cr diffusion in sapphire is smaller than the Cr diffusion in chrysoberyl or Ti in sapphire. The composition, stoichiometry, temperature, and pressure generally influence how atoms diffuse into different structures. Porosity, site energy, and ionic radii are also important determinants of diffusivity [13]. In our previous work, we suggested that the difference between Cr diffusion in sapphire and in chrysoberyl was due to the differences in their crystal structures. The Al^{3+} ions in sapphire are octahedrally coordinated by oxygen ions. Chromium diffusion in chrysoberyl, however, is structurally more difficult than in corundum since the Be^{2+} ions are tetrahedrally coordinated at interstitial sites [14].

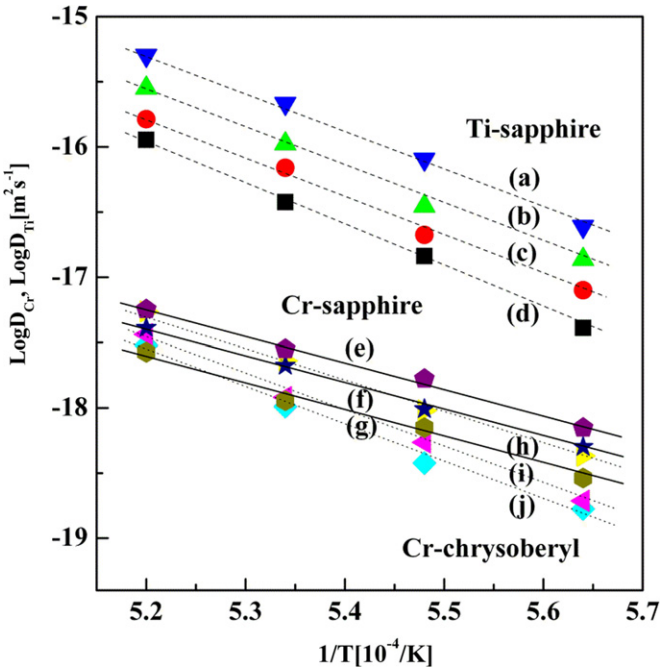

Fig. 9. Plot of Ti diffusions in synthetic sapphires (dashed lines) and Cr diffusions in natural sapphires (solid lines) and natural chrysoberyls (dotted lines). Dotted lines are the data from Ahn et al. [12] for Cr diffusion in natural chrysoberyl. Solid lines are the data from Ahn et al. [6] for Cr diffusion in natural sapphire. For Ti diffusion in synthetic sapphire: (a) irradiated, Ti-coated, and embedded in TiO_2/BeO powder; (b) irradiated, Ti-coated, and embedded in TiO_2 powder; (c) irradiated, non-coated, and embedded in TiO_2 powder; and (d) non-irradiated and embedded in TiO_2 powder. For Cr diffusion in natural sapphire: (e) irradiated, Cr-coated, and embedded in Cr_2O_3 powder; (f) irradiated, non-coated, and embedded in Cr_2O_3 powder; and (g) non-irradiated and embedded in Cr_2O_3 powder. For Cr diffusion in natural chrysoberyl: (h) electron beam irradiated, non-coated, and embedded in Cr_2O_3 powder; (i) proton beam irradiated, non-coated, and embedded in Cr_2O_3 powder; and (j) non-irradiated and embedded in Cr_2O_3 powder.

5. Conclusions

This study found that pre-treating samples by coating with Ti, irradiating with an electron beam, and embedding in a TiO_2/BeO mixture was the best method to diffuse titanium into sapphire. To increase the penetration of transition metals into the crystal lattice, we investigated several diffusion methods based on previous research (i.e., H^+ ion beam irradiation, electron beam irradiation, coating the crystal surface with metal, and embedding samples in a TiO_2/BeO mixture) [6,12]. Among these, embedding samples in a BeO/TiO_2 mixture resulted in the deepest diffusion. To adjust the cation balance in the corundum, Be^{2+} ions require Ti^{4+} ions, making Ti^{4+} ions follow Be^{2+} ion diffusion. To achieve ionic charge balance, the Ti^{4+} ions that diffused into the sapphire were coupled by adjacent Be^{2+} ions. Ti^{4+} ions can continuously diffuse into the sapphire lattice from the surface due to the concentration gradient.

In SEM analysis, we observed that few TiO_2 grains sintered onto the sapphire surface due to rapid cooling from 1673 K. The Cr_2O_3 crystals were angular, but TiO_2 crystals were amorphous. The difference between the TiO_2 and Cr_2O_3 crystals seen in the Ti and Cr diffusion experiments seems to be due to the cooling methods.

The Ti diffusivity data were compared with Cr diffusivity data from our previous study [6,12]. The Ti diffusivities in sapphire were considerably different from Cr in sapphire or chrysoberyl. There was an approximately single order

Table 2
Activation energies of diffusion in sapphire and chrysoberyl samples.

Conditions for diffusion of Cr or Ti	Activation energy (kJ/mol)
(a) Synthetic sapphire irradiated, Ti coated, and embedded in TiO_2/BeO powder	572.1 ± 18.5
(b) Synthetic sapphire irradiated, Ti coated, and embedded in TiO_2 powder	577.4 ± 23.3
(c) Synthetic sapphire irradiated, non-coated, and embedded in TiO_2 powder	582.4 ± 27.1
(d) Synthetic sapphire non-irradiated and embedded in TiO_2 powder	621.4 ± 12.4
(e) Natural sapphire irradiated, Cr coated, and embedded in Cr_2O_3 powder	385.7 ± 18.2
(f) Natural sapphire irradiated, non-coated, and embedded in Cr_2O_3 powder	401.0 ± 14.7
(g) Natural sapphire non-irradiated and embedded in Cr_2O_3 powder	405.9 ± 28.7
(h) Natural chrysoberyl electron beam irradiated, non-coated, and embedded in Cr_2O_3 powder	482.3 ± 18.2
(i) Natural chrysoberyl proton beam irradiated, non-coated, and embedded in Cr_2O_3 powder	545.4 ± 25.0
(j) Natural chrysoberyl non-irradiated and embedded in Cr_2O_3 powder	547.9 ± 36.8

difference in the diffusion coefficients (m^2s^{-1}) of Cr and Ti in non-irradiated sapphires at 1773 K. Therefore, we verified that Ti was able to diffuse into the sapphire lattice more easily than Cr due to the smaller radius. The slope of diffusivity, however, was lowest for Cr diffusion into sapphire, meaning that Cr diffusion into sapphire had the smallest activation energy.

Acknowledgments

This work was supported by the research fund of National Research Foundation of Korea grant number 2012-003926. The Gem and Jewelry Institute of Thailand provided sample analyses by LA-ICP-MS.

References

[1] F. Werfel, O. Brummer, Corundum structure oxides studied by XPS, Physica Scripta 28 (1983) 92.
[2] R.D. Shannon, Revised effective ionic radii and systematic studies of interatomic distances in halides and chalcogenides 32 (1976) 751Acta Crystallographica A 32 (1976) 751.
[3] P.F. Moulton, Spectroscopic and laser characteristics of Ti: Al_2O_3, Journal of the Optical Society of America B 3 (1986) 125.
[4] J.L. Emmett, K. Scarratt, S.F. McClure, T. Moses, T.R. Douthit, R. Hughes, S. Novak, J.E. Shigley, W. Wang, O. Bordelon, R.E. Kane, Beryllium diffusion of ruby and sapphire, Gems and Gemology (2003) 84.
[5] K. Nassau, The Physics and Chemistry of Color: The Fifteen Causes of Color, Wiley, New York, 1983.
[6] Y.K. Ahn, J.G. Seo, J.W. Park, Diffusion of chromium in sapphire: the effects of electron beam irradiation, Journal of Crystal Growth 326 (2011) 45.
[7] J.M. Rickman, H.M. Chan, M.P. Harmer, Grain boundary diffusion of Cr in pure and Y-doped alumina, Journal of the American Ceramic Society 90 (2007) 1551.
[8] F. Adam, B. Dupre, K. Kowalski, C. Gleitzer, J. Nowotny, Diffusion of Cr in CoO, Journal of Physics and Chemistry of Solids 56 (1995) 1063.
[9] W.D. Callister Jr., Materials Science and Engineering:An Introduction, seventh ed., Wiley, New York, 2007.
[10] B. Campbell, A. Mainwood, Radiation damage of diamond by electron and gamma irradiation, Physica Status Solidi A 181 (2009) 99.
[11] K.H. Lee, J.H. Crawford Jr., Electron centers in single-crystal Al_2O_3, Physical Review B 15 (980) (1977) 4065.
[12] Y.K. Ahn, J.G. Seo, J.W. Park, Diffusion of chromium in chrysoberyl, Journal of Crystal Growth 311 (2009) 3943.
[13] E. Dowty, Crystal-chemical factors affecting the mobility of ions in minerals, American Mineralogist 65 (1980) 174.
[14] E.F. Farrell, J.H. Fang, R.E. Newnham, Refinement of the chrysoberyl structure, American Mineralogist 48 (1963) 804.